

Lead isotope geochemical characteristics of Pb-Zn-Cu deposits on the southwestern margin of Tarim, and their significance

SHEN Nengping^{1*}, ZHANG Zhengwei¹, YOU Fuhua^{1,2}, PENG Jiantang¹, ZHU Xiaoqing¹, and XIAO Jiafei¹

¹ State Key Laboratory of Ore Deposit Geochemistry, Institute of Geochemistry, Chinese Academy of Sciences, Guiyang 550002, China

² Graduate University of Chinese Academy of Sciences, Beijing 100049, China

* Corresponding author, E-mail: shennengping@vip.gyig.ac.cn

Received May 3, 2012; accepted June 5, 2012

© Science Press and Institute of Geochemistry, CAS and Springer-Verlag Berlin Heidelberg 2012

Abstract The polymetallic (Pb, Zn, Cu, etc) ore belt on the southwestern margin of Tarim is one of the major regions with the greatest prospecting potential in Xinjiang. Reported in this paper are the lead isotope data for 66 sulfide samples (including 50 galena samples, 15 chalcopyrite samples and 1 pyrite sample) collected from such representative deposits as Tamu, Tiekelike, Kalangu, Abalieke, etc. in this ore belt. The Pb isotopic ratios of $^{206}\text{Pb}/^{204}\text{Pb}$, $^{207}\text{Pb}/^{204}\text{Pb}$ and $^{208}\text{Pb}/^{204}\text{Pb}$ in the galena samples range from 17.931 to 18.176, 15.609 to 15.818 and 38.197 to 38.944, with the average values of 18.017, 15.684 and 38.462, respectively. Those in the chalcopyrite samples range from 17.926 to 18.144, 15.598 to 15.628 and 38.171 to 38.583, with the average values of 18.020, 15.606 and 38.262, respectively. The pyrite sample has the Pb isotopic ratios of $^{206}\text{Pb}/^{204}\text{Pb}$, $^{207}\text{Pb}/^{204}\text{Pb}$ and $^{208}\text{Pb}/^{204}\text{Pb}$ to be 17.980, 15.604 and 38.145, respectively. In combination with the previous Pb isotope data for sulfides, it is found that there is only a slight variation in the Pb isotopic composition of galena, chalcopyrite, sphalerite and pyrite in the ore belt. However, there is some difference in Pb isotopic characteristics between galena and chalcopyrite, especially the Pb isotopic composition of galena shows an obvious linear correlation with some other relevant parameters (e.g. $\Delta\beta$ and $\Delta\gamma$). The comprehensive analysis suggested that lead in galena (maybe including sphalerite and pyrite) was derived principally from wall rocks and underlying basement, and that in chalcopyrite only originated from the basement. The single-stage model ages of these sulfides couldn't indicate the time limit of metallogenesis (Pb, Zn, Cu, etc.), and the positive linear correlations for the Pb isotopic composition of galena are of no single-stage and two-stage Pb-Pb isochron significance. Furthermore, there are significant differences in Pb isotopic composition characteristics between the genetic type of deposits in this polymetallic ore belt and the Mississippi Valley type (MVT). In addition, the authors also pointed out that there is a phenomenon of differentiation (not paragenesis) for lead and copper elements during the process of metallogenesis in this ore belt.

Key words lead isotope; lead source; Pb-Zn-Cu deposit; southwestern margin of Tarim

1 Introduction

The polymetallic (Pb, Zn, Cu, etc.) ore belt on the southwestern margin of Tarim is one of the major regions with the greatest prospecting potential in Xinjiang. It has attracted great attention of the broad masses of geological workers (Zhu Xinyou et al., 1997, 1998, 1999, 2000; Wang Dongbo et al., 2000; Wang Shulai et al., 2000, 2001, 2002; Kuang Wenlong et al., 2002a, b, c, 2003, 2005; Chang Xuesheng, 2003; Kuang Wenlong, 2003; Yin Jianping et al., 2003; Zhou Zhijian et al., 2004; Kuang Wenlong and Liu Wenwei, 2006; Li Boquan and Wang Jingbin, 2006; Yuan Bo, 2007; Hu Qingwen et al., 2007, 2008;

Feng Guangying et al., 2009; Yang Xiangrong et al., 2009a, b). As is known, this ore belt is located in a remote area, field investigations always encounter with great difficulties and annual working hours are limited, all these lead to a lower level of overall research degree. At present, there have been proposed the following cognitions concerning the genesis of ore deposits in this ore belt. In the 1950s the No.702 Team of Xinjiang Non-Ferrous Metals Company preliminarily explored this ore belt, considering that the ore deposits there belonged to the post-magmatic hydrothermal type. At the beginning of the 21st century new research results gave rise to a variety of hypotheses or viewpoints. Most researchers considered that they

should belong to the MVT ore deposits (Zhu Xinyou et al., 1997, 1998; Wang Shulai et al., 2001; Kuang Wenlong et al., 2002a, b, c, 2003, 2005). Hu Qingwen et al. (2007) thought that those ore deposits were of sea-floor hot brine exhalation origin. Yuan Bo (2007) held that they were the meso-epithermal vein-like ore deposits controlled jointly by strata and structures. Recently, Zhang Zhengwei et al. (2009) proposed that it was wise to explain the genesis of ore deposits in terms of the viewpoint of sedimentation-reworking since it fitted in with the concrete needs for ore prospecting. As for ore deposits of different genetic types, there are significant differences in their ore-forming materials. Therefore, how to distinguish the sources of ore-forming materials is one of the keys to constrain the genetic types of ore deposits, especially the sources of metallic elements (i.e., Pb, Zn, Cu, etc.) which are closely associated with metallogenesis. And the Pb isotopic composition is regarded as the most direct and effective approach to trace this type of ore-forming materials, thus finding wide applications in research on metallic to non-metallic ore deposits. In recent years, the authors have made a series of field geological investigations into and comprehensive research on the polymetallic ore belt on the southwestern margin of Tarim (starting from the Tiekelike Pb-Cu deposit in the north to the Tuokuziate Pb-Zn deposit in the south). In this paper sulfide mono-minerals (galena, chalcopyrite and pyrite) in this ore belt were selected as the research candidates, with an attempt to reveal the Pb isotope geochemical characteristics of this ore belt and the source of lead in ores, so as to further expound the sources of ore-forming materials and deepen our understanding of the genesis of ore deposits in this ore belt.

2 Regional geology and characteristics of typical ore deposits

The Pb-Zn-Cu polymetallic ore belt on the southwestern margin of Tarim is geotectonically located in the carbonate rock-distributed area at the juncture of the southwestern margin of the Tarim Basin with the West Kunlun orogenic belt, generally NNW-SSE extending (Fig. 1). At present, in this belt which is about 100 km long and 10 km wide there have been discovered more than 40 ore deposits (occurrences) and mineralization occurrences, all of which are hosted in the Late Paleozoic (Devonian, Carboniferous) strata. The Devonian system is a suite of light metamorphic marine terrigenous clastic rocks, and it includes two formations, i.e., the Middle Devonian Keziletuo Formation (D_2k) and the Upper Devonian Qizilafu Formation (D_3q). The Carboniferous system is relatively stable lithologically and it is generally composed of moderately thick carbonate rocks,

intercalated with minor clastic sedimentary rocks. This suite of strata includes five formations, which are named from the bottom to the top the Lower Carboniferous Kelitage Formation (C_1k), the Lower Carboniferous Heshilafu Formation (C_1h), the Middle Carboniferous Kalawuyi Formation (C_2k), the Middle Carboniferous Azigan Formation (C_2a) and the Upper Carboniferous Tahaqi Formation (C_3t). In the study area, in addition to the Devonian and Carboniferous strata in association with metallogenesis, there are also developed underlying Precambrian metamorphic and magmatic rocks and overlying Permian strata. The strata are relatively simple in composition. Additionally, from the Keziletuo Formation to the Permian system the main portions of various strata are all in conformable contact. The regional fault structures are mainly the Kegang fault zone (also called the Muzaling fault zone, the North Kudi fault, constituting the structural boundary between the Tarim plate and the West Kunlun structural zone), the Kaokuya fault zone (constituting the structural boundary between the Kashi depression and Tiekelike epicontinental fault uplifts), and at the same time, it serves as the frontal-edge fault of the pre-thrust nappe structure of West Kunlun Mountains) and the Keziletuo-Kusilafu fault zone (serving as the trailing-edge fault of the pre-thrust nappe structure of West Kunlun Mountains) (Zhang Zhengwei et al., 2009). These fault zones all show a NW-NNW strike and they not only control the development of sedimentary formations, but also probably control the distribution of the main Pb-Zn-Cu polymetallic ore deposits in the study area. Magmatic activities were extremely weak in this ore belt. With the exception of the small-scale eruption of Early Permian basaltic magmas in the Qimeigan and Qipan regions and the occurrence of some diabase dykes in the Kalangu and Abalieke regions, little has been reported about the distribution of other types of intrusive rocks and volcanic rocks. Therefore, most researchers considered that magmatic activities in the study area have nothing to do with the metallogenesis of those Pb-Zn ore deposits in the ore belt.

The Tamu, Tiekelike, Kalangu, Abalieke and other representative ore deposits reported in this study (Table 1) are relatively large in scale in the polymetallic ore belt situated on the southwestern margin of Tarim, and they possess all types of ore-forming element associations. In this ore belt those Pb-, Zn- and Cu-bearing orebodies are relatively complicated in form and most of them occur as stratoid, lenticular and veined orebodies in the Keziletuo, Kelitage or Heshilafu formations. The major metallic minerals include galena, sphalerite, chalcopyrite, and minor pyrite. On the near-ground surface or in the oxidation zone there exist some secondary minerals of Pb, Zn, and Cu. The gangue minerals are dominated by

dolomite, quartz, calcite, etc. In addition, the wall rock alterations in association with metallogenesis mainly include silicification, dolomitization, calcitization, etc.

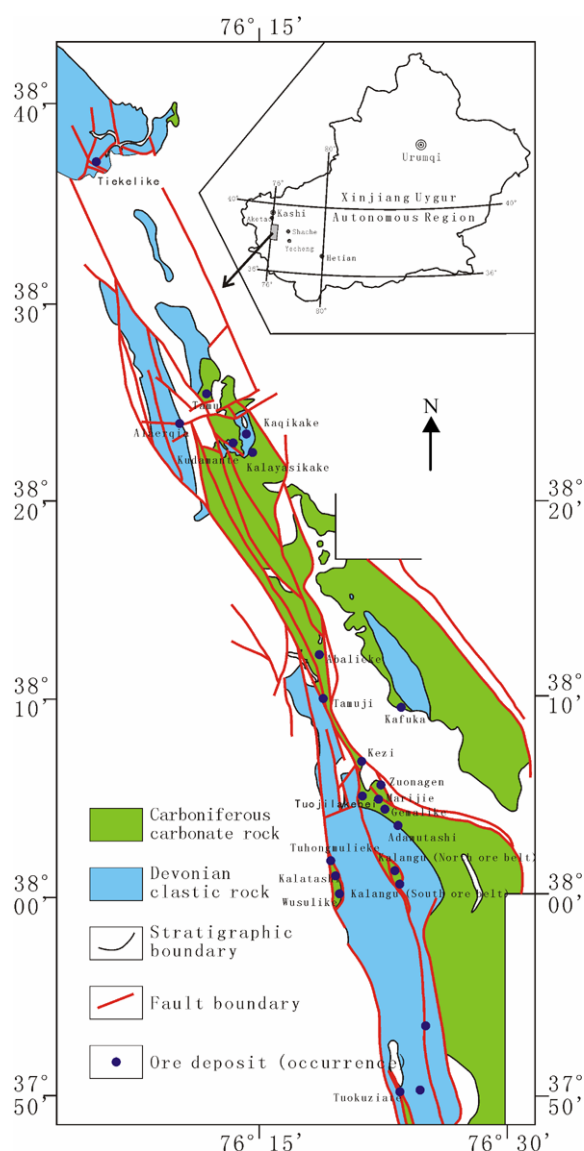


Fig. 1. The regional geological sketch map of the southwestern margin of Tarim (Revised after 1:100000 geological and mineral map, 2004). The solid and open symbols respectively represent the data obtained in this study and the data obtained by our predecessors. Different colors represent the corresponding ore deposits.

3 Sample collection and measurement

All the samples used in this study were collected from the fresh working surface of underground funnels of the representative Pb-Zn-Cu ore deposits in the polymetallic ore belt on the southwestern margin of Tarim. Firstly, the samples were ground as fine as 40–80 mesh in size in a steel hammer crusher, and impurities were picked out under a binocular microscope and then ground as fine as less than 200 mesh by means of an agate mortar.

Preparation of the samples for the measurement of Pb isotopic composition was accomplished at the Beijing Research Institute of Uranium Geology. The analytical procedure is described as follows: (1) A proper amount of sample was taken and weighed and put into a Teflon crucible, followed by adding hydrofluoric acid and perchloric acid for sample dissolution. After decomposition, the sample solution was evaporated till dryness. Then, hydrochloric acid was added to dissolve the sample further and the sample solution was evaporated till dryness. 0.5 N HBr was used to dissolve the sample for Pb separation. (2) The solution for dissolving the sample was poured into the pre-treated strongly alkaline ion exchange resin for Pb separation, and then 0.5 N HBr was used to elute the resin and then 2 N HCl was used to elute the resin again. Finally, 6 N HCl was used for extraction, and the extracted solution was evaporated till dryness for mass spectrometric measurement. (3) The measurement of Pb isotopic ratios was accomplished on the ISOPROBE-T Model thermal ionization mass spectrometer. The $^{208}\text{Pb}/^{206}\text{Pb}$ measurement accuracy for 1 μg Pb is better than 0.005%. In addition, this measurement was monitored by using the international standard NBS981 and the results of measurement are $^{208}\text{Pb}/^{206}\text{Pb}=2.1660624$, $^{207}\text{Pb}/^{206}\text{Pb}=0.9145628$ and $^{204}\text{Pb}/^{206}\text{Pb}=0.0590837$, respectively.

4 Measurement results and analysis

Listed in Table 1 are the Pb isotopic compositions and characteristic values of 66 sulfide mono-mineral samples analyzed in this study (50 galena samples, 15 chalcopyrite samples and 1 pyrite sample). Statistics data showed that the Pb isotopic ratios of $^{206}\text{Pb}/^{204}\text{Pb}$, $^{207}\text{Pb}/^{204}\text{Pb}$ and $^{208}\text{Pb}/^{204}\text{Pb}$ in the galena samples are 17.931–18.176 (averaging 18.017), 15.609–15.818 (averaging 15.684) and 38.197–38.944 (averaging 38.462), respectively; those in the chalcopyrite samples are 17.926–18.144 (averaging 18.020), 15.598–15.628 (averaging 15.606) and 38.171–38.583 (averaging 38.262), respectively. Involved in this study is only one pyrite sample which was collected from the Tiekelike Pb-Cu deposit, whose Pb isotopic ratios are 17.980, 15.604 and 38.145, respectively. These 66 galena, chalcopyrite and pyrite samples are characterized by relatively unanimous variations in Pb isotopic composition (Fig. 2), but relative to the galena samples the Pb isotopic ratios of $^{207}\text{Pb}/^{204}\text{Pb}$ and $^{208}\text{Pb}/^{204}\text{Pb}$ in the chalcopyrite samples are low. It can also be seen at the same time that the Pb isotopic composition of the galena samples displays an obvious linear distribution. This linear distribution can be divided into two trends: one is constituted by the samples collected from the Tiekelike, Tamu and Kalayashikake ore deposits and the other

Table 1 The Pb isotopic compositions and characteristic values of sulfides from Pb-Zn-Cu deposits in the polymetallic ore belt on the southwestern margin of Tarim

Sequence No.	Sample No.	Sample source	Mineral	$^{206}\text{Pb}/^{204}\text{Pb} \pm 2\sigma$	$^{207}\text{Pb}/^{204}\text{Pb} \pm 2\sigma$	$^{208}\text{Pb}/^{204}\text{Pb} \pm 2\sigma$	T	μ	Th/U	V ₁	V ₂	$\Delta\alpha$	$\Delta\beta$	$\Delta\gamma$
1	TKLK-10	Tiekelike	Galena	18.028 ± 0.001	15.697 ± 0.001	38.439 ± 0.003	553	9.71	3.95	58.3	41.9	57.6	24.8	36.7
2	TKLK-23	Tiekelike	Galena	18.080 ± 0.001	15.680 ± 0.001	38.474 ± 0.002	498	9.66	3.94	60.5	43.7	60.6	23.6	37.6
3	TKLK-28	Tiekelike	Galena	18.021 ± 0.001	15.687 ± 0.001	38.397 ± 0.003	547	9.69	3.94	57.1	41.8	57.2	24.1	35.6
4	TKLK-32	Tiekelike	Galena	18.067 ± 0.001	15.752 ± 0.004	38.611 ± 0.004	587	9.81	4.02	63.5	43.1	59.9	28.3	41.3
5	TKLK-33	Tiekelike	Chalcopyrite	18.000 ± 0.001	15.628 ± 0.001	38.583 ± 0.002	494	9.57	4.02	61.1	37.3	55.9	20.3	40.6
6	TKLK-37	Tiekelike	Galena	18.029 ± 0.002	15.705 ± 0.002	38.463 ± 0.005	561	9.72	3.97	58.9	41.8	57.6	25.3	37.3
7	TKLK-38	Tiekelike	Galena	18.036 ± 0.002	15.714 ± 0.002	38.484 ± 0.004	566	9.74	3.97	59.6	42.2	58.0	25.9	37.9
8	TKLK-914	No. 6 adit, Tiekelike	Galena	18.032 ± 0.002	15.688 ± 0.002	38.414 ± 0.005	540	9.69	3.94	57.8	42.2	57.8	24.2	36.0
9	TKLK-916	No. 6 adit, Tiekelike	Chalcopyrite	18.013 ± 0.001	15.603 ± 0.001	38.201 ± 0.002	456	9.52	3.84	52.2	41.7	56.7	18.6	30.3
10	TKLK-917	No. 6 adit, Tiekelike	Pyrite	17.980 ± 0.001	15.604 ± 0.001	38.145 ± 0.002	481	9.52	3.84	50.0	40.7	54.8	18.7	28.8
11	TKLK-918	No. 6 adit, Tiekelike	Galena	18.035 ± 0.002	15.693 ± 0.002	38.435 ± 0.004	544	9.70	3.95	58.4	42.2	58.0	24.5	36.6
12	TKLK-919	No. 6 adit, Tiekelike	Chalcopyrite	18.141 ± 0.001	15.615 ± 0.001	38.404 ± 0.002	379	9.52	3.87	60.4	46.0	64.2	19.4	35.8
13	TKLK-921A	No. 6 adit, Tiekelike	Galena	18.020 ± 0.002	15.692 ± 0.002	38.407 ± 0.004	561	9.72	3.96	58.8	42.0	57.8	25.3	37.2
14	TKLK-921B	No. 6 adit, Tiekelike	Galena	18.055 ± 0.001	15.735 ± 0.001	38.549 ± 0.003	577	9.78	3.99	61.7	42.9	59.2	27.2	39.7
15	TKLK-921C	No. 6 adit, Tiekelike	Galena	17.963 ± 0.001	15.642 ± 0.000	38.250 ± 0.001	536	9.60	3.90	52.1	39.5	53.8	21.2	31.6
16	TKLK-922	No. 6 adit, Tiekelike	Chalcopyrite	17.977 ± 0.001	15.598 ± 0.001	38.349 ± 0.002	476	9.51	3.93	54.8	38.1	54.6	18.3	34.3
17	TM-807	Tamu	Galena	17.992 ± 0.001	15.638 ± 0.001	38.316 ± 0.003	512	9.59	3.91	54.4	40.1	55.5	20.9	33.4
18	TM-809	Tamu	Galena	17.994 ± 0.002	15.643 ± 0.002	38.323 ± 0.005	516	9.60	3.91	54.6	40.3	55.6	21.2	33.6
19	TM-810	Tamu	Galena	18.022 ± 0.001	15.677 ± 0.001	38.453 ± 0.003	535	9.67	3.96	58.5	41.0	57.2	23.4	37.1
20	TM-813	Tamu	Galena	18.044 ± 0.003	15.706 ± 0.004	38.514 ± 0.010	552	9.72	3.98	60.5	42.0	58.5	25.3	38.7
21	TM-814	Tamu	Galena	18.050 ± 0.001	15.716 ± 0.001	38.547 ± 0.003	559	9.74	3.99	61.5	42.2	58.9	26.0	39.6
22	TM-25	Tamu	Galena	18.010 ± 0.001	15.661 ± 0.001	38.380 ± 0.002	525	9.63	3.94	56.4	40.8	56.5	22.4	35.1
23	TM-37-1	Tamu	Galena	18.012 ± 0.001	15.663 ± 0.001	38.377 ± 0.001	526	9.64	3.93	56.4	41.0	56.6	22.5	35.0
24	TM-901	Line 2 at 2480 m level, Tamu	Galena	17.970 ± 0.002	15.610 ± 0.001	38.197 ± 0.004	495	9.54	3.87	51.0	39.8	54.2	19.1	30.2
25	TM-902	Line 2 at 2480 m level, Tamu	Galena	17.987 ± 0.001	15.631 ± 0.001	38.268 ± 0.002	507	9.58	3.89	53.1	40.3	55.2	20.4	32.1
26	TM-916	Line 2 at 2480 m level, Tamu	Galena	18.008 ± 0.001	15.661 ± 0.001	38.369 ± 0.002	526	9.63	3.93	56.1	40.9	56.4	22.4	34.8
27	TM-918	Line 2 at 2480 m level, Tamu	Galena	17.983 ± 0.001	15.627 ± 0.001	38.263 ± 0.002	505	9.57	3.89	52.9	40.0	54.9	20.2	32.0
28	TM-929	Line 0-1 at 2420 m level, Tamu	Galena	18.013 ± 0.001	15.665 ± 0.001	38.392 ± 0.001	527	9.64	3.94	56.8	40.9	56.7	22.7	35.4
29	TM-932	Level 2480 m, Tamu	Galena	17.997 ± 0.001	15.640 ± 0.001	38.326 ± 0.002	510	9.59	3.91	54.8	40.3	55.8	21.0	33.7

(to be continued)

Table 1 (continued)

Sequence No.	Sample No.	Sample source	Mineral	$^{206}\text{Pb}/^{204}\text{Pb} \pm 2\sigma$	$^{207}\text{Pb}/^{204}\text{Pb} \pm 2\sigma$	$^{208}\text{Pb}/^{204}\text{Pb} \pm 2\sigma$	T	μ	Th/U	V ₁	V ₂	$\Delta\alpha$	$\Delta\beta$	$\Delta\gamma$
		Tamu												
30	TM-936	Level 2620 m, Tamu	Galena	17.974 ± 0.001	15.620 ± 0.001	38.252 ± 0.001	504	9.56	3.89	52.4	39.6	54.4	19.7	31.7
31	TM-938	Level 2480 m, Tamu	Galena	18.032 ± 0.004	15.694 ± 0.004	38.483 ± 0.011	547	9.70	3.97	59.5	41.5	57.8	24.6	37.9
32	TM-944	Level 2510 m, Tamu	Galena	18.007 ± 0.002	15.655 ± 0.002	38.336 ± 0.006	520	9.62	3.92	55.3	41.0	56.3	22.0	33.9
33	TM-947	Level 2510 m, Tamu	Galena	18.024 ± 0.002	15.679 ± 0.002	38.437 ± 0.004	536	9.67	3.95	58.2	41.3	57.3	23.6	36.6
34	TM-948	Level 2510 m, Tamu	Galena	18.049 ± 0.002	15.712 ± 0.002	38.532 ± 0.004	555	9.73	3.99	61.1	42.2	58.8	25.7	39.2
35	ALEQ-901	Alaerqia	Galena	17.975 ± 0.002	15.679 ± 0.002	38.493 ± 0.004	570	9.68	4.00	58.2	38.3	54.5	23.6	38.2
36	ALEQ-903	Alaerqia	Galena	17.956 ± 0.001	15.656 ± 0.001	38.426 ± 0.002	557	9.63	3.98	56.1	37.5	53.4	22.1	36.3
37	ALEQ-915	Alaerqia	Galena	18.023 ± 0.002	15.746 ± 0.002	38.719 ± 0.006	610	9.81	4.09	65.0	39.6	57.3	28.0	44.2
38	ALEQ-918	Alaerqia	Galena	17.989 ± 0.001	15.698 ± 0.001	38.560 ± 0.003	581	9.71	4.03	60.2	38.6	55.3	24.8	40.0
39	ABLK-708	Abalieke	Chalcopyrite	17.966 ± 0.001	15.600 ± 0.001	38.172 ± 0.001	486	9.52	3.85	50.2	39.6	53.9	18.4	29.5
40	ABLK-709	Abalieke	Chalcopyrite	18.046 ± 0.001	15.599 ± 0.001	38.186 ± 0.002	428	9.50	3.82	52.7	43.4	58.6	18.4	29.9
41	ABLK-713	Abalieke	Chalcopyrite	17.978 ± 0.001	15.601 ± 0.001	38.195 ± 0.003	479	9.52	3.86	51.1	40.0	54.6	18.5	30.1
42	ABLK-720	Abalieke	Galena	17.994 ± 0.002	15.652 ± 0.002	38.357 ± 0.005	526	9.62	3.93	55.4	40.1	55.6	21.8	34.5
43	ABLK-727	Abalieke	Chalcopyrite	17.972 ± 0.001	15.607 ± 0.001	38.210 ± 0.003	490	9.53	3.87	51.3	39.6	54.3	18.9	30.5
44	ABLK-829	Abalieke	Chalcopyrite	18.096 ± 0.001	15.604 ± 0.001	38.171 ± 0.003	399	9.51	3.78	53.6	46.1	61.6	18.7	29.5
45	ABLK-903A	Abalieke	Chalcopyrite	18.144 ± 0.001	15.608 ± 0.001	38.221 ± 0.002	369	9.51	3.78	56.0	48.0	64.4	18.9	30.8
46	ABLK-917	Abalieke	Galena	17.969 ± 0.003	15.646 ± 0.004	38.325 ± 0.01	537	9.61	3.93	54.0	39.1	54.1	21.4	33.6
47	ABLK-933	Abalieke	Chalcopyrite	18.019 ± 0.001	15.609 ± 0.001	38.251 ± 0.002	459	9.53	3.86	53.5	41.5	57.0	19.0	31.6
48	ABLK-934	Abalieke	Chalcopyrite	18.058 ± 0.001	15.599 ± 0.001	38.220 ± 0.002	425	9.53	3.84	55.2	44.1	60.2	19.2	31.9
49	ABLK-937	Abalieke	Chalcopyrite	17.946 ± 0.001	15.614 ± 0.001	38.280 ± 0.003	516	9.55	3.92	52.3	37.7	52.8	19.3	32.4
50	THMLK-914	Tuhongmuliieke	Galena	17.986 ± 0.001	15.676 ± 0.001	38.454 ± 0.002	559	9.67	3.98	57.6	39.2	55.1	23.4	37.1
51	THMLK-N907	Tuhongmuliieke	Galena	17.931 ± 0.004	15.644 ± 0.003	38.348 ± 0.006	561	9.61	3.96	53.6	36.9	51.9	21.3	34.2
52	THMLK-N907	Tuhongmuliieke	Chalcopyrite	17.926 ± 0.001	15.601 ± 0.001	38.216 ± 0.001	516	9.53	3.90	50.3	37.2	51.6	18.5	30.7
53	THMLK-N909	Tuhongmuliieke	Galena	17.951 ± 0.001	15.609 ± 0.001	38.279 ± 0.003	507	9.54	3.91	52.4	37.9	53.1	19.0	32.4
54	THMLK-N915	Tuhongmuliieke	Galena	17.976 ± 0.003	15.693 ± 0.004	38.569 ± 0.009	584	9.70	4.04	60.1	37.8	54.5	24.5	40.2
55	KLY-901	Kalayasikake	Chalcopyrite	18.022 ± 0.001	15.610 ± 0.001	38.266 ± 0.002	458	9.53	3.87	54.0	41.6	57.2	19.1	32.0
56	KLY-915	Kalayasikake	Galena	18.124 ± 0.002	15.751 ± 0.001	38.664 ± 0.003	547	9.80	4.01	66.2	45.3	63.2	28.3	42.8
57	KLY-919	Kalayasikake	Galena	18.152 ± 0.001	15.794 ± 0.002	38.859 ± 0.004	575	9.88	4.09	71.7	45.5	64.9	31.1	48.0
58	KLY-921	Kalayasikake	Galena	18.176 ± 0.002	15.818 ± 0.002	38.944 ± 0.006	585	9.93	4.11	74.4	46.3	66.3	32.7	50.3
59	KLY-926	Kalayasikake	Galena	18.064 ± 0.002	15.704 ± 0.001	38.535 ± 0.003	536	9.71	3.98	61.6	42.8	59.7	25.2	39.3
60	KLY-927	Kalayasikake	Galena	18.034 ± 0.002	15.684 ± 0.002	38.462 ± 0.004	534	9.68	3.96	59.0	41.6	57.9	23.9	37.3
61	KLIG-12	Kalangu	Galena	18.048 ± 0.002	15.702 ± 0.002	38.550 ± 0.004	545	9.71	3.99	61.5	41.8	58.8	25.1	39.7
62	KLIG-1-901	Kalangu	Galena	18.014 ± 0.004	15.716 ± 0.005	38.645 ± 0.012	584	9.75	4.06	62.9	39.3	56.8	26.0	42.3
63	KLIGX-902	Kalangu	Galena	17.994 ± 0.004	15.705 ± 0.004	38.556 ± 0.009	585	9.73	4.03	60.3	39.1	55.6	25.3	39.9
64	KLIGX-905	Kalangu	Galena	17.975 ± 0.001	15.675 ± 0.001	38.490 ± 0.002	565	9.67	4.00	58.2	38.2	54.5	23.3	38.1
65	WSLK-01	Wusuliike	Galena	18.017 ± 0.001	15.747 ± 0.002	38.736 ± 0.004	616	9.81	4.10	65.2	39.2	56.9	28.0	44.7
66	WSLK-03	Wusuliike	Galena	17.946 ± 0.001	15.645 ± 0.001	38.418 ± 0.002	552	9.61	3.98	55.7	36.9	52.8	21.4	36.1

Note: The GeoKit software package (Lu Yuanfa, 2004) was used to calculate the parameters. T was taken as 250 Ma.

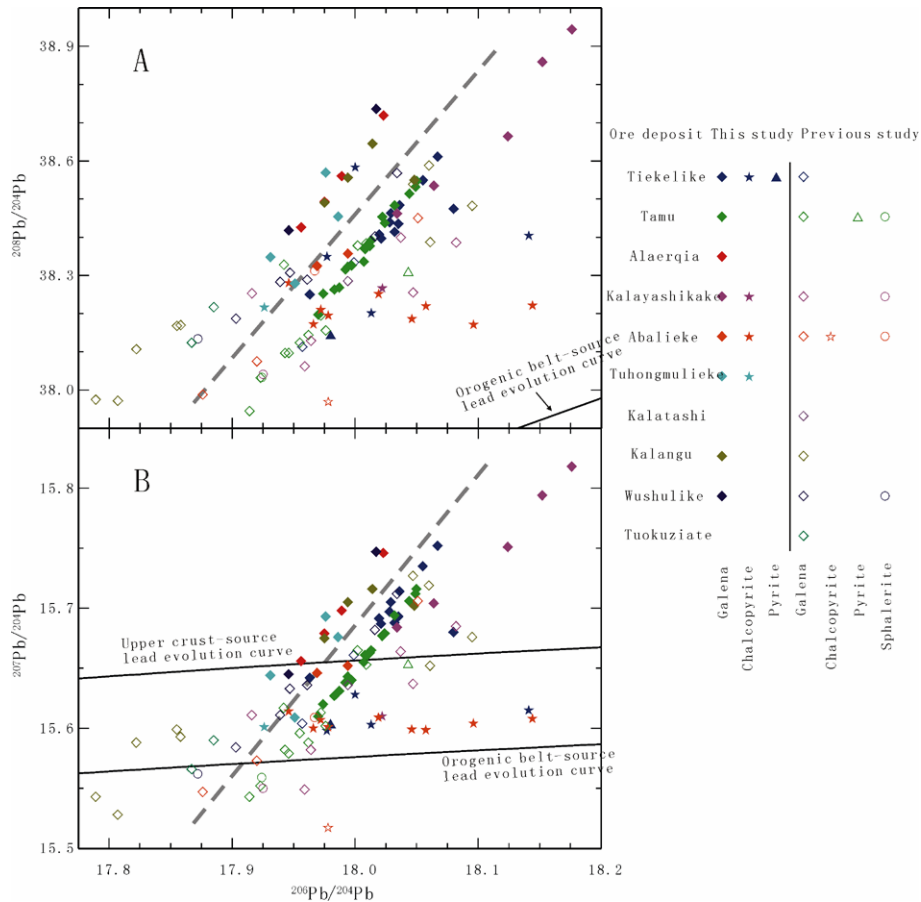


Fig. 2. The Pb isotopic compositions of sulfides from Pb-Zn-Cu deposits in the polymetallic ore belt on the southwestern margin of Tarim (the data of lead evolution curve adopted from Zartman and Doe, 1981).

by the samples collected from the Alaerqia, Tuhongmulieke and Wushulike ore deposits. Moreover, on the whole, the Pb isotopic composition of the chalcopyrite sample is relatively scattered, though there is a nearly horizontal distribution trend (Fig. 2B). However, the values of its correlation coefficient are small.

In the previous studies our predecessors also acquired the Pb isotope data from sulfides in the ore deposits in the polymetallic ore belt situated on the southwestern margin of Tarim. By comparing those data with the equivalent data obtained in this study (not including those from iron ore deposits), it is found that in the previous data (Wang Dongbo et al., 2000; Kuang Wenlong et al., 2002a; Kuang Wenlong and Liu Wenwei, 2006) one pyrite sample (KB604) collected from the Kalayashikake Pb-Zn deposit possesses a unique Pb isotopic composition (Wang Dongbo et al., 2000), which has the lowest ratios of $^{208}\text{Pb}/^{204}\text{Pb}$ (only 37.513), $^{206}\text{Pb}/^{204}\text{Pb}$ (17.712) and $^{207}\text{Pb}/^{204}\text{Pb}$ (15.358). With the exception of that pyrite sample (it is not included in the following discussion), comparisons of 66 sets of Pb isotope data obtained in this study with previous 46 sets of Pb isotope data (including the data of 40 galena samples, 4 sphalerite samples, one chalcopyrite sample, and one pyrite

sample) revealed the following differences (Fig. 2): (1) The Pb isotopic composition data of previous galena samples are mainly located at the low-value end. As shown in the comprehensive figure, the two linear distribution trends are more obvious; (2) Among the previous Pb isotope data, only one chalcopyrite sample taken from Abalieke Cu-Pb deposit has a relatively low $^{208}\text{Pb}/^{204}\text{Pb}$ ratio as can be verified by its Pb isotopic composition which did not fall within the field of Pb isotopic composition of chalcopyrite acquired in this study; and (3) There is a relatively significant difference in Pb isotopic composition between galena samples collected in this work from the Kalangu Pb-Zn deposit and those collected by our predecessors from the same Pb-Zn deposit. The data points of the galena samples are distributed on both the left and right sides of the Pb isotopic composition linear distribution field.

5 Discussion

5.1 Sources of Pb and ore-forming metals

Generally speaking, the contents of U and Th in sulfides are very low, so the amount of radiogenic lead

resultant from the decay of U and Th is low, thus its influence on the Pb isotopic composition can be ignored (Zhang Ligang, 1992; Zhang Qian et al., 2000). The Pb isotopic composition of sulfide mono-minerals in the polymetallic ore belt situated on the southwestern margin of Tarim, which was determined by us and our predecessors, needs no correction. That is to say, the Pb isotopic composition truly represents the initial Pb isotopic ratio at the time when various sulfides were formed.

One can make use of the plumbotectonics model (Zartman and Doe, 1981) to constrain the source of Pb. As shown on the $^{206}\text{Pb}/^{204}\text{Pb}$ - $^{208}\text{Pb}/^{204}\text{Pb}$ diagram (Fig. 2A), the Pb isotopic composition data for all sulfides obtained in this study and previous research work are all projected on the left upper side of the Pb evolution curve of the orogenic belt and on the right side of the extension of the Pb evolution curve of the lower crust. On the $^{206}\text{Pb}/^{204}\text{Pb}$ - $^{207}\text{Pb}/^{204}\text{Pb}$ diagram (Fig. 2B) the Pb isotopic composition data of sulfides measured in this work are all projected on the upper side of the Pb evolution curve of the orogenic belt, and on both sides of the Pb evolution curve of the upper crust. The projective points of the most majority of pyrite samples are located near the upper side of the Pb evolution curve of the orogenic belt. However, the previous data partly fall below the Pb evolution curve of the orogenic belt and are distributed near this Pb evolution curve. The projective points of the samples are almost of linear distribution, but this line shows no isochron tendency, indicating that the samples only represent the characteristics of source regions with different μ values. This implies that there would be a possibility of imperfect mixing of normal lead in the different source regions. In addition, the fact that the projective points fall above the crustal evolution curve implies that the lead is in the environment where $^{232}\text{Th}/^{204}\text{Pb}$ and $^{238}\text{U}/^{204}\text{Pb}$ are increasing for long. So the above Pb isotopic composition characteristics indicate the lead sources are not only the upper crust, but also some other source regions, for example, the basement of the West Kunlun orogenic belt (Zhu Bingquan et al., 1998).

Zhu Bingquan et al. (1998) carried out a deep-going study on a lot of ore lead and rock lead isotopes. Variations in Th and Pb isotopic composition and the interrelationship between the Th and Pb isotopic compositions and the U and Pb isotopic compositions can provide abundant information about the geological processes and material sources. In order to stand out the variation relationship between Pb isotopic compositions and eliminate the influence of time factor, Zhu Bingquan et al. (1998) expressed the three kinds of Pb isotopic compositions as the relative deviations to the primary mantle lead, i.e., $\Delta\alpha$, $\Delta\beta$ and $\Delta\gamma$, and also proposed the $\Delta\beta$ - $\Delta\gamma$ genetic classification

diagram of ore lead isotopes. This classification scheme has found wide applications in China. These diagrammatized parameters need the comparative calculation of metallogenic epoch data and contemporaneous mantle lead. Because of the lack of reliable metallogenic epoch data, the calculation had to rely on the data on Hercynian hydrothermal metallogenesis in this ore belt (Henan Institute of Geological Survey, 2006), in combination with the important tectono-transformation metallogenic epoch at the end of Permian in this region (Zhang Zhengwei et al., 2009). Moreover, as it is considered that the errors involved in metallogenic age have little influence on the acquired parameters, the metallogenic age, T , is 250 Ma. On the basis of the relative deviations for sulfide lead from the representative ore deposits in the polymetallic ore belt situated on the southwestern margin of Tarim and contemporaneous mantle lead (Table 1), $\Delta\alpha$, $\Delta\beta$ and $\Delta\gamma$ were calculated to be 43.6–66.3 (averaging 55.5), 13.0–32.7 (averaging 21.2) and 23.4–50.3 (averaging 33.8), respectively. It can be seen that they just vary over a small range. On the $\Delta\beta$ - $\Delta\gamma$ genetic classification diagram (Fig. 3) the projective points fall mainly in the field of the subduction-source lead resultant from mixing of the upper crust-source lead and the mantle-source lead, and only few projective points fall in the field of upper crust-source lead and orogenic belt-source lead. And both $\Delta\beta$ and $\Delta\gamma$ for galena samples have extremely obvious linear correlations. However, in the polymetallic ore belt on the southwestern margin of Tarim there has been found no sign of intense magmatic activities, and previous researchers also considered that the Pb, Zn, Cu polymetallic metallogenesis had nothing to do with magmatic activities (Zhu Xinyou et al., 1997; Kuang Wenlong et al., 2002a, b). Therefore, these distribution characteristics further imply that during the process of metallogenesis in this region a part of lead would come from the basement. In addition, the characteristic values of vectors for the lead isotopes in those sulfide samples, V_1 and V_2 , vary over a relatively small range, to be 40.9–74.4 (averaging 54.8) and 31.8–48.0 (averaging 40.1), respectively. As can be seen from Fig. 4, the projective points of chalcopyrite samples are also relatively scattered, whereas those of galena samples display a linear distribution trend.

In addition, the μ values of a total of 112 sulfide samples are within the range of 9.35–9.93 with an average value of 9.60. Of the sulfide samples, 49 samples have μ values of less than 9.58 (including all the 15 chalcopyrite samples studied in this work). The results indicated that there exist low radiogenic deep-source lead in some samples, especially in the chalcopyrite samples. Meanwhile, the model Th/U ratios of those samples vary over a large range, from 3.74 to

4.11, with an average value of 3.92, and the data of only 32 samples are lower than the upper crust average value (3.88) (Zartman and Hainess, 1988) while the data of most of the samples are higher than that value, indicating that they were not formed completely in the upper crust. Comparisons revealed that the Th/U ratios of those samples are higher than those in the upper crust but lower than those in the lower crust (Wedepohl, 1987), equivalent to the Th/U ratio of shales (4.1), far greater than the Th/U ratio of carbonate rocks (0.77), implying that the material source seems to be somewhat related to sandy shale strata. Orebodies of sedimentary strata-bound Pb-Zn deposits in this ore belt are generally hosted in carbonate strata. If ore-forming materials were derived from sandy shales, there would occur the processes of ore-forming material extraction, migration and precipitation. The above processes can not be traced merely on the basis of Pb isotopic analysis. Moreover, in terms of the analysis of regional stratigraphy data (Henan Institute of Geological Survey, 2006), it can be seen that the Pb isotopic ratios ($^{206}\text{Pb}/^{204}\text{Pb}$, $^{207}\text{Pb}/^{204}\text{Pb}$ and $^{208}\text{Pb}/^{204}\text{Pb}$) of Carboniferous carbonate rocks and detrital sandy shales in southwestern Tarim are within the ranges of 18.03–18.29, 15.59–15.65 and 38.12–38.46, respectively. The Pb isotopic values of sulfide minerals determined in this work are within the above ranges (with the exception of a few samples, Table 1), implicating that the source of metallic elements in sulfides in ore-forming materials seems to be related, to some extent, to the ore-host strata or other Carboniferous strata. Therefore, the lead component in the metallic ore belt situated on the southwestern margin of Tarim may be derived mainly from ore-host rocks and underlying basement. The fact that the Pb isotopic composition and some characteristic values of the galena samples show linear correlations also provides strong evidence for the above deduction.

5.2 Relationship between model age and metallogenic epoch

The single-stage Pb model ages of 112 sulfide samples taken from the polymetallic ore belt on the southwestern margin of Tarim vary over a range of 369.0–615.5 Ma (averaging 517.1 ± 47.3 Ma). Of the 112 sulfide samples, there are 90 galena samples whose Pb model ages are within the range of 431.6–615.5 Ma (averaging 531.1 ± 35.9 Ma), and 16 chalcopyrite samples whose model ages vary over a range of 369.0–516.4 Ma (averaging 450.4 ± 48.9 Ma). As compared to chalcopyrite samples, the model ages of galena samples vary over a large range, and the average value is 80 Ma larger than the chalcopyrite samples. All those model ages are larger than the boundary age between the Upper Carboniferous

Pennsylvanian and the Lower Carboniferous Mississippian (318.1 ± 1.3 Ma), also larger than the boundary age between the Carboniferous system and the Devonian system (359.2 ± 2.5 Ma). Even as compared to the boundary age between the Middle and Upper Devonian series (385.3 ± 2.6 Ma), there are only three samples whose model ages are slightly low, that is to say, those model ages are obviously greater than the ages of the ore-host strata of Pb, Zn and Cu ore deposits (D_2k , C_1k , C_1h). So, those ages are of no geochronological significance, thus unable to indicate the time limit of metallogenesis of Pb, Zn, Cu and other metals in this ore belt.

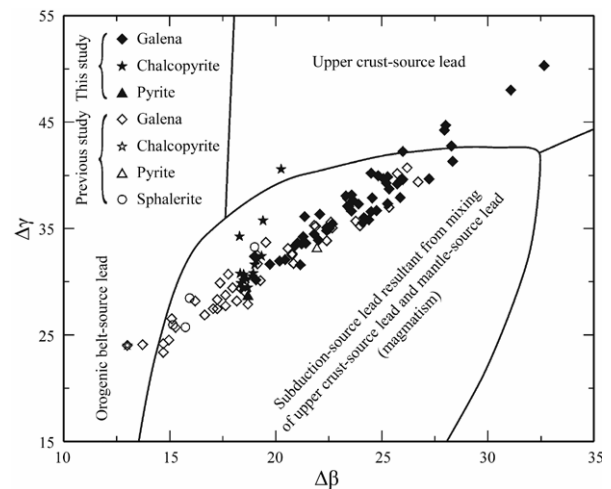


Fig. 3. $\Delta\beta$ - $\Delta\gamma$ diagram of the genetic classification of Pb isotopic compositions of sulfides from Pb-Zn-Cu deposits in the polymetallic ore belt on the southwestern margin of Tarim (The original map is after Zhu Bingquan et al., 1998).

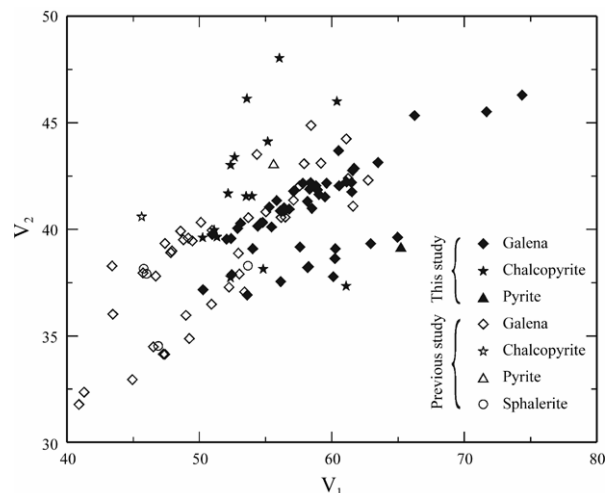


Fig. 4. Diagram of V_1 and V_2 characteristic values of Pb isotopic compositions of sulfides from Pb-Zn-Cu deposits in the polymetallic ore belt on the southwestern margin of Tarim.

It is worthy of note that on the $^{206}\text{Pb}/^{204}\text{Pb}$ - $^{208}\text{Pb}/^{204}\text{Pb}$ and $^{206}\text{Pb}/^{204}\text{Pb}$ - $^{207}\text{Pb}/^{204}\text{Pb}$ diagrams (Fig.

2A, B) the Pb isotopic composition of galena samples displays two sets of linear distribution. Such linear distribution characteristics are more precise than the linear correlations for the Pb isotopic composition of sulfides in a large number of metallic ore deposits, for example, the Xujiashan stibnite ore deposit in Hebei Province (Shen Nengping et al., 2008). As can be seen from Fig. 2B, the best linear correlations are shown for the Pb isotopic composition of 29 galena samples from the Tamu Zn-Pb deposit, with the linear equation: $y=1.224x-6.38$ (the correlation coefficient is as high as up to 0.98). If the metallogenic age (t) is calculated by using the $^{206}\text{Pb}/^{204}\text{Pb}$ - $^{207}\text{Pb}/^{204}\text{Pb}$ isochron (the slope $R=\frac{e^{\lambda_{235}t_1}-1}{137.88(e^{\lambda_{238}t_1}-1)}$), the metallogenic age

obtained would be extremely unreasonable (5520 Ma), indicating that this linear relationship is of no single-stage Pb-Pb isochron significance (Peng Jiantang et al., 2000). Using the formula

$$R=\frac{e^{\lambda_{235}t_1}-e^{\lambda_{238}t_2}}{137.88(e^{\lambda_{238}t_1}-e^{\lambda_{238}t_2})}$$

to calculate the two-stage Pb model ages, one can obtain two age values: t_1 and t_2 (assuming $t_1>t_2$): t_1 represents the time of first mineralization or the time of rock formation (the age of source materials), and t_2 represents the time when anomalous lead is precipitated finally, i.e., the time of second mineralization. That is to say, the radiogenic lead was produced during the time period of $t_1\rightarrow t_2$. From this one can take the single-stage model age of 29 galena samples from the Tamu ore deposit (the data of 18 samples determined in this work are listed in Table 1) as t_2 into the equation and obtain $t_1=5435\pm 5$ Ma. This age value goes so far as to be larger than the age of the Earth, indicating that this linear relationship is of no two-stage Pb isochron significance either. A linear arrangement is shown on the $^{206}\text{Pb}/^{204}\text{Pb}$ - $^{208}\text{Pb}/^{204}\text{Pb}$ and $^{206}\text{Pb}/^{204}\text{Pb}$ - $^{207}\text{Pb}/^{204}\text{Pb}$ diagrams, but the slope of the straight line has nothing to do with the age. This case is usually considered to be the result that mixing to two kinds of normal Pb leads to the production of anomalous lead. Moreover, slight variations in Pb isotopic composition and older model ages than those of ore-host rocks are characteristic of type-B lead. This type of lead represents the lead buried in the strata after it broke away from the U-Th source, then it was involved in the process of sedimentation-precipitation. So, the positive linear correlations for the Pb isotopic composition of galena samples from the metallogenic ore belt on the southwestern margin of Tarim may have resulted from mixing of two kinds of lead sources, thus of no single-stage and two-stage Pb-Pb isochron significance.

5.3 Comparative study

Many researchers classified the ore deposit type

dominated by the Pb-Zn deposits in the polymetallic ore belt on the southwestern margin of Tarim as the MVT (Zhu Xinyou et al., 1997, 1998; Wang Shulai et al., 2001; Kuang Wenlong et al., 2002a, b, c, 2003, 2005). Scholars both at home and abroad have done much work on the Pb isotopic composition of the MVT deposits. For example, Brown and Maryland (1970) pointed out in their studies that there was a significant difference in Pb isotopic composition between the MVT and ordinary hydrothermal deposits. The most obvious feature is that the former is enriched in radiogenic lead. Leach et al. (2005) have summarized the results of research on the Pb isotopic composition of sulfide samples collected from 30 MVT ore deposits (or districts) and drawn similar conclusions. Although some researchers pointed out that the Pb isotopic composition characteristics of the MVT Pb-Zn deposits are indicative of the existence of J-type, B-type and normal lead, it is suggested that the lead is of multi-source mixing (Cannon et al., 1963), i.e., the “confounding” of many kinds of isotopic compositions. In this paper the authors collected and made statistical analysis of the Pb isotope data for some typical MVT ore deposits (or districts) published by our predecessors (listed in Table 2 for the convenience of comparison). Through comparisons it was found that the Pb isotopic ratios of $^{206}\text{Pb}/^{204}\text{Pb}$ in sulfides from the polymetallic ore belt on the southwestern margin of Tarim are obviously low, all not exceeding 18.2, but, with the exception of few cases (just like the Pine Point), the equivalent ratios of sulfides in the MVT ore deposits (or districts) are generally higher than 20, even up to 24 or more (Heyl et al., 1966). The case is true for the ratios of $^{208}\text{Pb}/^{204}\text{Pb}$. The ratios of $^{208}\text{Pb}/^{204}\text{Pb}$ in most sulfides from the polymetallic ore belt on the southwestern margin of Tarim do not exceed 38.7, whereas the average values of sulfide samples from the typical MVT ore deposits (or districts) mostly exceed 40, though those of some individual samples are close to 44 (Heyl et al., 1966). Relatively speaking, there is no significant difference in $^{207}\text{Pb}/^{204}\text{Pb}$ between a large number of ore deposits in the polymetallic ore belt and the most majority of the MVT ore deposits (or districts), though the latter’s is still higher than the former’s. It can be seen clearly merely from the above comparisons that the most majority of the MVT ore deposits (or districts) possess unique Pb isotopic compositions and are highly enriched in U and Th. Our predecessors called such lead as the “Mississippi-type lead” (Zhu Bingquan et al., 1998). As can be seen clearly from Table 1, the Pb isotopic composition of sulfides from the ore deposits in the polymetallic ore belt on the southwestern margin of Tarim is characterized by the concentrated distribution of numerical values, a narrow fluctuation range, and a significant difference from the Missis-

issippi-type lead. So, it can at least be judged from the ore Pb isotopic composition that these ore deposits have no comparability with the MVT ore deposits.

5.4 The phenomena of Pb, Zn and Cu paragenesis and differentiation

Lead, Zn, Cu and other elements in the polymetallic ore belt on the southwestern margin of Tarim can form not only independent ore deposits (occurrences), but also paragenetic (associated) ore deposits (occurrences), in most of which a certain element serves as the important ore-forming element and other elements serve as subordinate elements to coexist, be associated with the important one or to be separated from it.

Regionally, the contents of ore-forming elements such as Cu, Pb and Zn are high in the west but low in the east of the profile, almost having no correlation with the strata but being closely related to the tectonic background. The contents of the three elements in the regional strata follow an increasing order of $Zn > Pb > Cu$, indicating a geological background characterized by enrichment in Zn and Pb but depletion in Cu. As compared to the Clarke values of the crust, there is a tendency of separation of Cu from Pb and Zn, implying there is some difference in geological background of metallogenesis between Pb and Zn, and Cu. The high background anomalies of the ore-forming elements only occur in the local specific positions of the strata (Henan Institute of Geological Survey, 2006).

In the typical mining area, Cu and Pb orebodies in the Tiekeli-like Pb-Cu deposit and Abalieke Cu-Pb deposit show a phenomenon of relatively obvious separation. The exposed strata in the Tiekeli-like mining area are dominated by the Middle Devonian Keziletuo Formation. Orebodies occur in the first lithological section and the lithological assemblage is divided into three layers: yellowish-brown thin-layered siltstone in the lower layer, grayish-white quartz sandstone interbedded with calcareous sandstone and limestone in the middle layer, and limonite-bearing mineralized quartz sandstone in the upper layer. Mineralization is observed mainly in the calcareous cemented grayish-white, medium-grained quartz sandstone in the middle layer. The ore-forming elements show a phenomenon of mineralization zoning, with copper mineralization in the lower part. Orebodies are stratiform and stratoid and their occurrence is generally in accord with that of the strata. In some locations the orebodies intersect with the rock strata. The ores are composed mainly of fine-grained sparse mineralized chalcopyrite, with a minor amount of pyrite. In the upper part is developed Pb mineralization. In the Abalieke mining area are mainly exposed the Devo-

nian-Carboniferous strata, and the ore-bearing strata are represented by the Lower Carboniferous Heshilafu Formation, which can be divided into four lithological sections from the bottom to the top: (1) light purple argillaceous conglomerate-bearing sandstone, sandstone and siltstone; (2) a set of carbonate rock formations, composed of yellowish-brown to grayish-yellow brecciated limy dolomite intercalated with minor amounts of coarse sandstone and thin-layered quartz fine conglomerate. This dolomite layer underwent different degrees of limonitization, and orebodies are hosted in the tectono-crushed zone; (3) dark grey thin-layered siltstone interbedded with thin-layered limestone and greyish-green, thin-layered siltstone intercalated with argillaceous limestone in the upper part; and (4) grey to light grey limestone, mostly with silicification and calcitization. As viewed from the current analysis of exploration results in the mining area, Cu, Pb and Zn mineralization is restricted to the tectono-crushed zone of the second lithological section. The occurrence of orebodies is generally in accord with that of the rock strata. Element zoning is characterized by the distribution of Pb in the upper part and that of Cu in the lower part. Stratoid and veined orebodies are dominant, with a branching-compositing phenomenon (Zhang Zhengwei et al., 2009). It is just in correspondence to the geological phenomenon of zoning of the above-mentioned ore-forming elements, reflecting that there is also spatial zonation with respect to Pb isotopic composition. As is shown in Fig. 2, the distribution of the projective points of galena shows such a linear tendency as to be right-inclined and go upwards, while the distribution of the projective points of chalcopyrite shows a nearly horizontal linear tendency, with an evolution tendency of source regions with almost identical μ values (As compared to galena, the μ values are relatively low and are concentrated in the stable range of 9.50–9.55), implying that the evolution direction of material sources of chalcopyrite shows a tendency of separation from galena. In addition, the projective points of chalcopyrite all fall in between the orogenic-source lead evolution curve and the upper crust-source lead evolution curve, reflecting the Pb isotopic composition characteristics of a single basement source region.

There would be some difference in metallogenic epoch between chalcopyrite and galena. The Pb isotope model age of chalcopyrite is generally lower than that of galena, though it is older than the forming time of Upper Devonian series in the lowest part of the ore-bearing strata. The geological fact that this Pb model age is older than the forming time of ore-host rocks reflects the possibility of contamination by older lead and the process of contamination seem to be related to the later process of galena mineralization. According to the metallogenesis geochronology data

we have obtained, the Re and Os isotope data of chalcopyrite from the copper orebodies of the Abalieke ore deposit yielded an isochron age of 331.3 ± 5.2 Ma, corresponding to Hercynian time (Zhang Zhengwei et al., 2011), while the Re and Os isotope data from chalcopyrite in Pb orebodies of the Tiekelike ore deposit yielded a model age of 210 ± 10 Ma, corresponding to Indosinian time (the data have not yet been published officially). Although this model age needs to be further verified, it is in correspondence to the geological explanation of metallogenesis at that time (Zhang Zhengwei et al., 2009). It is deduced from this that there are some significant differences between chalcopyrite samples and galena samples in the distribution characteristics of Pb isotopic composition of sulfides in the polymetallic ore belt on the southwestern margin of Tarim and related characteristic values. The lead in galena is derived mainly from two sources while that in chalcopyrite is derived mainly from the basement. The mineralization time of Pb and Cu is of no synchronicity. As viewed from the angle of element

paragenesis and differentiation, the two elements Pb and Cu in this ore belt mainly show a tendency of differentiation in the process of metallogenesis.

6 Conclusions

Through a comprehensive analysis of the Pb isotopic compositions of sulfide samples taken from the representative ore deposits in the Pb, Zn, Cu polymetallic ore belt on the southwestern margin of Tarim, the following cognitions have been obtained:

(1) The Pb isotopic compositions of four kinds of sulfide samples including galena, chalcopyrite, sphalerite and pyrite from this ore belt vary over a small range, and the Pb isotopic compositions of galena samples show obvious linear correlations. Their Pb isotopic characteristics indicate that the lead in galena (probably also including sphalerite and pyrite) is derived mainly from ore-host rocks and the underlying basement, while that in chalcopyrite is derived mainly from the basement.

Table 2 Comparisons of the Pb isotopic compositions of galena from some typical MVT ore deposits or districts with those of sulfides in the West Kunlun area

Ore deposit (or district)	Sample number	$^{206}\text{Pb}/^{204}\text{Pb}$	$^{207}\text{Pb}/^{204}\text{Pb}$	$^{208}\text{Pb}/^{204}\text{Pb}$	Data source
Pine Point	37	17.170–18.187 (18.121)	15.570–15.578 (15.574)	38.153–38.203 (38.169)	Cumming et al., 1990
Viburnum trend in Southeast Missouri	14	21.31–22.66 (22.11)	16.00–16.28 (16.15)	41.07–41.92 (41.46)	Russell and Farquhar, 1960
Old Pb belt in Southeast Missouri	6	20.750–21.600 (21.068)	15.850–15.926 (15.879)	39.720–40.824 (40.128)	Goldhaber et al., 1995
Southeast Missouri	6	20.749–21.052 (21.560)	15.581–15.913 (15.826)	39.585–40.556 (39.911)	Doe and Delevaux, 1972
Tri-state district	3	21.901–22.210 (22.018)	15.920–15.960 (15.934)	41.072–41.330 (41.159)	Goldhaber et al., 1995
Central Appalachians	9	18.505–19.055 (18.645)	15.614–15.683 (15.632)	38.388–39.029 (38.631)	Kesler et al., 1994a
Southern Appalachian	6	18.501–19.415 (19.138)	15.650–15.734 (15.698)	37.985–39.534 (39.064)	Kesler et al., 1994b
Upper Mississippi Valley (Wisconsin-Illinois-Iowa)	19	20.83–24.44 (22.54)	15.96–16.33 (16.15)	40.45–43.95 (42.31)	Heyl et al., 1966
Illinois-Kentucky	8	19.91–21.01 (20.36)	15.80–15.98 (15.90)	39.92–40.64 (40.27)	Heyl et al., 1966
Southeast Missouri	131	19.96–21.46 (20.81)	15.65–16.19 (15.97)	39.10–41.02 (40.08)	Heyl et al., 1974
Buick mine in Southeast Missouri	8	20.435–21.749 (21.145)	15.817–15.919 (15.878)	39.283–40.733 (40.031)	Sverjensky et al., 1979
Tiekelike	16	17.963–18.141 (18.030)	15.598–15.752 (15.671)	38.145–38.611 (38.413)	This study
Tamu	18	17.970–18.050 (18.009)	15.610–15.716 (15.661)	38.197–38.547 (38.376)	This study
Alaerqia	4	17.956–18.023 (17.986)	15.656–15.746 (15.695)	38.426–38.719 (38.550)	This study
Abalieke	11	17.946–18.144 (18.017)	15.599–15.652 (15.613)	38.171–38.357 (38.235)	This study
Tuhongmulieke	5	17.926–17.986 (17.954)	15.601–15.693 (15.645)	38.216–38.569 (38.373)	This study
Kalayasikake	6	18.022–18.176 (18.095)	15.610–15.818 (15.727)	38.266–38.944 (38.622)	This study
Kalangu	4	17.975–18.048 (18.008)	15.675–15.716 (15.700)	38.490–38.645 (38.560)	This study
Wusulike	2	17.946–18.017 (17.982)	15.645–15.747 (15.696)	38.418–38.736 (38.577)	This study

Note: The data in the brackets are the average values.

(2) The single-stage Pb model ages of sulfide samples from this ore belt can not indicate the time limit of metallogenesis of Pb, Zn, Cu and other metallic elements. At the same time, the linear correlations for the Pb isotopic compositions of galena samples are of no single-stage and two-stage Pb-Pb isochron significance.

(3) The Pb isotopic composition characteristics of sulfides in various representative ore deposits in this ore belt are obviously different from the isotopic composition characteristics of the Mississippi-type lead. As viewed, at least, from the angle of ore lead isotopic composition, those ore deposits do not genetically belong to the MVT.

(4) The lead in galena and chalcopyrite in this ore belt comes from different sources and there exists a time difference for the metallogenesis of Pb and Cu. All this indicates that in the process of their metallogenesis both the elements Pb and Cu are characterized by differentiation instead of paragenesis.

Acknowledgements In the field work the authors were given great support and help by general engineer Men Guangqian with the Ya Xing Mineral Resources Group Ltd. Co., engineer Zhang Hui from the Tiekeli-like Pb-Cu ore deposit, general manager Liu Jie and engineer Zhang Zhengshun from Tamu Pb-Zn ore deposit, Guixin Mineral Resources Development Ltd. Co., and director Li Fuliang with the Abalieke Cu-Pb Ore Dressing Plant. In laboratory analysis and measurement the authors also were given great support and help by Mrs. Liu Mu with Beijing Research Institute of Uranium Geology. In the preparation of the manuscript of this paper the authors exchanged ideas and made beneficial discussion with Dr. Yang Xiangrong with Xinjiang University. Prof. Zhu Bingquan with the Guangzhou Institute of Geochemistry, Chinese Academy of Sciences and Prof. Zhang Qian with the Institute of Geochemistry, Chinese Academy of Sciences, carefully reviewed the manuscript of this paper and made valuable comments. Here the authors wish to extend their sincere thanks to them all. This research project was financially supported jointly by the National Natural Science Foundation of China (No. 40903021), the Funding Project for Western Doctors of “Light of Western China” under the Talents Cultivation Program sponsored by the Chinese Academy of Sciences, the “Eleventh Five-Year Plan” Key Project of National Science and Technology Supporting Plan (2006BAB07B04-04), the Innovation Project of the Chinese Academy of Sciences (KZCX2-YW-107-6) and the Research Project of the State Key Laboratory of Ore Deposit Geochemistry.

References

- Brown J.S. and Maryland T. (1970) Mississippi Valley-type lead-zinc ores: A review and sequel to the “Behre Symposium” [J]. *Mineralium Deposita*. **5**, 103–119.
- Cannon R.S., Pierce Jr A.P., and Dekevaux M.H. (1963) Lead isotope variation with growth zoning in a galena crystal [J]. *Science*. **142**, 574–576.
- Chang Xuesheng (2003) Metallogenic characteristics and ore prospects of lead-zinc deposit in East Kunlun area, Xinjiang [J]. *Xinjiang Non-Ferrous Metallurgy*. **26**, 2–8 (in Chinese).
- Cumming G.L., Kyle J.R., and Sangster D.F. (1990) Pine point: A case history of lead isotope homogeneity in a Mississippi Valley-type district [J]. *Economic Geology*. **85**, 133–144.
- Doe B.R. and Delevaux M.H. (1972) Source of lead in Southeast Missouri galena ores [J]. *Economic Geology*. **67**, 409–425.
- Dong Yongguan, Guo Kunyi, Liao Shenbing, Xiao Huiliang, and Wang Tao (2006) Geological and geochemical characteristics of the Kekuxilik lead-zinc ore deposit, West Kunlun, Xinjiang [J]. *Acta Geologica Sinica*. **80**, 1730–1738 (in Chinese with English abstract).
- Feng Guangying, Liu Shen, Peng Jiantang, Zhang Zhengwei, Qi Huawen, Zhu Xiaoqing, Xiao Jifeng, and Wang Changhua (2009) Characteristics of fluid inclusions from Tamu-Kalangu lead-zinc metallogenic belt, Xinjiang [J]. *Journal of Jilin University (Earth Science Edition)*. **39**, 406–414 (in Chinese with English abstract).
- Goldhaber M.B., Church S.E., Doe B.R., Aleinikoff J.N., Brannon J.C., Podosek F.A., Mosier E.L., Taylor C.D., and Gent C.A. (1995) Lead and sulfur isotope investigation of Paleozoic sedimentary rocks from the southern Midcontinent of the United States: Implications for paleohydrology and ore genesis of the Southeast Missouri lead belts [J]. *Economic Geology*. **90**, 1875–1910.
- Henan Institute of Geological Survey (2006) *Geological Map of the P.R.C. (1:250000 scale geological map in Yingjisha County)* [R]. J43C002003.
- Heyl A.V., Delevaux M.H., Zartman R.E., and Brock M.R. (1966) Isotopic study of galenas from the upper Mississippi Valley, the Illinois-Kentucky, and some Appalachian Valley mineral districts [J]. *Economic Geology*. **61**, 933–961.
- Heyl A.V., Landis G.P., and Zartman R.E. (1974) Isotopic evidence for the origin of Mississippi Valley-type mineral deposits: A review [J]. *Economic Geology*. **69**, 992–1006.
- Hu Qingwen, Liu Honglin, and Zhu Hongying (2008) Research on ore forming conditions of Pb-Zn-Cu-(Ag-Co) mine in Tamu-Kalangu [J]. *Non-Ferrous Metallurgy*. **60**, 11–16 (in Chinese with English abstract).
- Hu Qingwen, Zhu Hongying, and Zhou Shenhua (2007) Regional ore-controlling conditions of the Tamu-Kalangu Pb-Zn (Cu) ore zone, Xinjiang [J]. *Mineral Resources and Geology*. **21**, 551–554 (in Chinese with English abstract).
- Kesler S.E., Appold M.S., Cumming G.L., and Krstic D. (1994a) Lead isotope geochemistry of Mississippi Valley-type mineralization in the Central Appalachians [J]. *Economic Geology*. **89**, 1492–1500.
- Kesler S.E., Cumming G.L., Krstic D., and Appold M.S. (1994b) Lead isotope geochemistry of Mississippi Valley-type deposits of the Southern Appalachians [J]. *Economic Geology*. **89**, 307–321.

- Kuang Wenlong and Liu Wenwei (2006) *Analysis of Minerogenetic Conditions and Predication of Prospective Area of Mississippi Valley-type Pb-Zn Deposits in Western Kunlun Region* [M]. pp.1–119. Geological Publishing House, Beijing (in Chinese).
- Kuang Wenlong, Gao Zhenquan, Yin Jianping, Zhu Ziqiang, and Liu Shihua (2002a) Study on metallogenetic process of Tamu MVT type lead-zinc ore deposit and the source of metallogenetic material in west of Kunlun [J]. *Bulletin Mineralogy, Petrology and Geochemistry*. **21**, 253–257 (in Chinese with English abstract).
- Kuang Wenlong, Gu Desheng, Liu Jishun, and Liu Wenwei (2005) A probe into fluid inclusions' characteristics of MVT deposits: Western Kunlun district in Xinjiang (China) [J]. *Non-Ferrous Mining and Metallurgy*. **21**, 1–5 (in Chinese with English abstract).
- Kuang Wenlong, Liu Jishun, Zhu Ziqiang, and Liu Shihua (2002b) Metallogenesis of Kalangu MVT lead-zinc deposit and sources of minerogenetic materials in western Kunlun [J]. *Geotectonica et Metallogenia*. **26**, 423–428 (in Chinese with English abstract).
- Kuang Wenlong, Liu Shihua, Liu Jishun, and Zhu Ziqiang (2002c) A probe into Kalangu MVT lead-zinc deposit's minerogenetic process and the source of minerogenetic material in West Kunlun [J]. *World Geology*. **21**, 340–346 (in Chinese with English abstract).
- Kuang Wenlong (2003) *Study on Minerogenetic Conditions and Model of the Mississippi Valley-type Pb-Zn Deposits in the Western Kunlun Region* [D]. pp.1–158. Doctor's Degree Paper, Central South University, Changsha (in Chinese with English abstract).
- Kuang Wenlong, Liu Jishun, Zhu Ziqiang, and Liu Shihua (2003) Minerogenetic mechanism of lead-zinc deposits in southwestern Tarim [J]. *Xinjiang Geology*. **21**, 136–140 (in Chinese with English abstract).
- Leach D.L., Sangster D.F., Kelley K.D., Large R.R., Garven G., Allen C.R., Gutzmer J., and Walters S. (2005) Sediment-hosted lead-zinc deposits: A global perspective [J]. *Economic Geology* (100th Anniversary). 561–607.
- Li Boqian and Wang Jingbin (2006) *Lead-zinc Deposits in Xinjiang, China* [M]. pp.1–171. Geological Publishing House, Beijing (in Chinese with English abstract).
- Liu Deqian, Tang Yanling, and Zhou Ruhong (2005) *Copper Deposits and Nickel Deposits in Xinjiang, China* [M]. pp.1–360. Geological Publishing House, Beijing (in Chinese with English abstract).
- Lu Yuanfa (2004) Geokit—A geochemical toolkit for Microsoft Excel [J]. *Geochimica*. **33**, 459–464 (in Chinese with English abstract).
- Peng Jiantang, Hu Ruizhong, and Su Wenchao (2000) Lead isotopic composition of ores in the antimony deposits at the southern margin of the Yangtze massif and its geological implications [J]. *Geology-Geochemistry*. **28**, 43–47 (in Chinese with English abstract).
- Shen Nengping, Peng Jiantang, Yuan Shunda, Zhang Dongliang, and Hu Ruizhong (2008) Lead isotope compositions and its significance for ore-forming material of the Xujiashan antimony deposit, Hubei Province [J]. *Acta Mineralogica Sinica*. **28**, 169–176 (in Chinese with English abstract).
- Sverjensky D.A., Rye D.M., and Doe B.R. (1979) The lead and sulfur isotopic compositions of galena from a Mississippi Valley-type deposit in the New Lead Belt, Southeast Missouri [J]. *Economic Geology*. **74**, 149–153.
- Wang Dongbo, Zhu Xinyou, and Wang Shulai (2000) *Study on Minerogenetic Conditions and Evaluation for the Tamu-Kalangu Pb-Zn Ore Belt* [M]. pp.1–83. Beijing Institute of Geology for Mineral Resources, Beijing (in Chinese).
- Wang Shulai, Wang Dongbo, and Zhu Xinyou (2000) Ore-searching prospect analysis of gold (copper) deposits in the western Kunlun area, Xinjiang autonomous region [J]. *Contributions to Geology and Mineral Resources Research*. **15**, 224–229 (in Chinese with English abstract).
- Wang Shulai, Wang Dongbo, and Zhu Xinyou (2001) The fluid inclusion in MVT lead-zinc deposit in southwest margin of Tarim [J]. *Mineral Resources and Geology*. **15**, 238–242 (in Chinese with English abstract).
- Wang Shulai, Wang Dongbo, Zhu Xinyou, Wang Jingbin, and Peng Shengling (2002) Ore-fluid geochemistry of Tamu-Kala Pb-Zn deposit in Xinjiang [J]. *Geology-Geochemistry*. **30**, 34–39 (in Chinese with English abstract).
- Wedepohl K.H. (1978) *Handbook of Geochemistry* (Vol. v/1) [M]. Springer, Berlin Heidelberg, New York.
- Yang Xiangrong, Peng Jiantang, Hu Ruizhong, Qi Huawen, and Liu Shen (2009a) Characteristics and genesis of ore tube structure of Tamu zinc-lead deposit, southwest margin of Tarim basin, Xinjiang [J]. *Acta Petrologica Sinica*. **25**, 977–983 (in Chinese with English abstract).
- Yang Xiaorong, Peng Jiantang, Hu Ruizhong, Qi Huawen, and Liu Shen (2009b) Fluid characteristic and ore genesis of Tamu lead and zinc ore deposit, Xinjiang [J]. *Geochimica*. **38**, 536–548 (in Chinese with English abstract).
- Yin Jianping, Tian Peiren, Qi Xuexiang, and Chen Keqiang (2003) Characteristics of geology and geochemistry of ore-bearing formation in Tamu-Kalangu lead-zinc-copper ore belts in western Kunlun mountain [J]. *Geoscience*. **17**, 143–150 (in Chinese with English abstract).
- Yuan Bo (2007) *Study of Geological Characteristics and Enrichment Regularities of Mineralization of Kalangu, Tamu Lead-zinc Deposits, West Kunlun, Xinjiang Province* [D]. pp.1–84. Changchun: Master's Degree Paper, Jilin University, Changchun (in Chinese with English abstract).
- Zartman R.E. and Doe B.R. (1981) Plumbotectonics—The model [J]. *Tectonophysics*. **75**, 135–162.
- Zartman R.E. and Haines S.M. (1988) The plumbotectonic model for Pb isotopic systematics among major terrestrial reservoirs—A case for bi-directional transport [J]. *Geochimica et Cosmochimica Acta*. **52**, 1327–1339.
- Zhang Ligang (1992) Present status and aspects of lead isotope geology [J]. *Geology and Prospecting*. **28**, 21–29 (in Chinese with English abstract).
- Zhang Qian, Pan Jiayong, and Shao Shuxun (2000) An interpretation of ore lead sources from lead isotopic compositions of some ore deposits in China [J]. *Geochimica*. **29**, 231–238 (in Chinese with English abstract).
- Zhang Zhengwei, Peng Jiantang, Xiao Jiafeng, Zhu Xiaoqing, Shen Nengping, Zhang Zhongshan, and You Fuhua (2009) Regional metallotectonics of the lead-zinc deposits zone in southwestern margin of the Tarim plate [J]. *Bulletin of Mineralogy, Petrology and Geochemistry*. **28**, 318–329 (in Chinese with English abstract).
- Zhang Zhengwei, Qi Liang, Shen Nengping, You Fuhua, Zhang Zhongshan, and Zhou Lingjie (2011) Re-Os isotopic dating of chalcopyrite from the Abalieke copper-lead deposits in west Kunlun, China [J]. *Acta Petrologica Sinica*. **27**, 3123–3128 (in Chinese with English abstract).
- Zhou Zhijian, Zheng Zhigang, and Chen Shiping (2004) Metallogenetic feature and prospecting direction of Taka lead and zinc ore field, western Kunlun, Xinjiang [J]. *Mineral Resources and Geology*. **18**, 128–133

(in Chinese with English abstract).

Zhu Bingquan, Li Xianhua, Dai Tongmu, Chen Yuwei, Fan Shikun, Gui Xuntang, and Wang Huifeng (1998) *Theory and Application of Isotopic Systematics in Earth Sciences With Discussion on Crustal Evolution of the Continent in China* [M], pp.1–330. Science Press, Beijing (in Chinese).

Zhu Xinyou, Wang Dongbo, and Wang Shulai (1997) Geology of the Tamu-Kalangu MVT Pb-Zn belt, Xinjiang [J]. *Geological Exploration for Non-Ferrous Metals*. **6**, 202–207 (in Chinese with English abstract).

Zhu Xinyou, Wang Dongbo, and Wang Shulai (1998) Geology and sulfur

isotope geochemistry of the Tamu-Kalangu lead-zinc deposits, Akto County, Xinjiang [J]. *Mineral Deposits*. **17**, 204–214 (in Chinese with English abstract).

Zhu Xinyou, Wang Dongbo, and Wang Shulai (1999) Potential for prospecting of Pb-Zn deposits on the western margin of Tarim Basin in Xinjiang [J]. *Geological Exploration for Non-ferrous Metals*. **8**, 413–416 (in Chinese with English abstract).

Zhu Xinyou, Wang Dongbo, and Wang Shulai (2000) The characteristics of ore-bodies, Tamu-Kalangu lead-zinc deposit, Arketao County, Xinjiang [J]. *Geology and Prospecting*. **36**, 32–35 (in Chinese with English abstract).